Characterization of copper corrosion products originated in simulated uterine fluids and on packaged intrauterine devices

J. M. BASTIDAS, N. MORA, E. CANO, J. L. POLO
Centro Nacional de Investigaciones Metalúrgicas (CSIC), Avda. Gregorio del Amo 8, 28040 Madrid, Spain

This paper studies the characterization of corrosion products originated after 1 and 12 weeks' immersion of copper specimens in simulated uterine fluids at pH 6.3 and 8.0 and at 37 °C temperature. The experimental techniques used were X-ray photo-electron spectroscopy, scanning electron microscopy, and energy dispersive X-ray. The compounds found were calcite ($CaCO_3$), calcium phosphate, cuprite (Cu_2O) and copper hydroxide ($Cu(OH)_2$). The morphology of corrosion products was a non-uniform, layer showing some paths through which copper ions can be released. In parallel, corrosion products formed on packaged, unused copper-containing intrauterine devices (IUD) were analyzed. Cuprite (Cu_2O) and chalcocite (Cu_2S) were the main species identified.

1. Introduction

It is known that the anti-fertility effect of an intrauterine device (IUD) can be improved if a copper wire is used to encase the stem of the device [1]. Though the mechanism of the contraceptive action of copper-containing IUDs is unclear, one hypothesis is that a copper-containing IUD may be effective as a result of the dissolution of the copper into uterine secretions and the formation of cupric ions, which lead to the inactivation of sperm and the suppression of myometrial contractions [2, 3]. A sterile inflammation that is enhanced by copper has also been hypothesized [1].

Available information seems to indicate an inverse relationship between the surface area of copper on IUDs and pregnancy rates [2–7]. Clinical studies have indicated that the average copper release rate after 3 years of use, depending on IUD type, is around 25 μg/day [8]. Circumstances that obstruct copper release may have a negative influence on IUD effectiveness. Thus, the presence of extensive calcite ($CaCO_3$) deposits covering the copper wire on these devices has been associated with accidental pregnancies [9]. Despite this, the influence of corrosion products formed on the copper surface in IUDs is a poorly studied subject.

Little information is available about the acute and subacute toxicity of copper released from copper devices. Copper, as a heavy metal, is toxic to the developing blastocyst and to sperm [3]. However, IUDs containing copper wire do not seem to have a direct toxic effect on the blastocyst since proteins in uterine secretions may provide protection against the free copper ions [10]. In this sense, copper is preferable to other metals such as iron, nickel, zinc, gold, silver and stainless steel [7, 11].

The original red color of copper on an IUD can change during storage and/or transportation before the device is used. The red color of copper is associated with cuprite (Cu_2O), which is an extremely thin film that forms spontaneously when a clean copper surface is exposed to air at room temperature [12, 13]. Thus, to answer the question as to whether a copper IUD can be used when the copper surface is covered by a dark layer is of practical importance [8, 14].

The aim of this paper is to characterize the corrosion products formed at early stages (after 1 and 12 weeks) on copper specimens immersed in simulated uterine fluids at two pH values. Another aim of the paper is to characterize the thin dark colored layer formed on copper on IUDs after 30 months storage at room temperature.

2. Materials and methods

Copper specimens with a chemical composition (wt %): 0.009 Sn, < 0.001 As, < 0.001 Bi, 0.003 Ni, < 0.001 Fe, 0.015 Pb, < 0.001 Mn, 0.019 P, < 0.0005 Ag, < 0.001 S, < 0.005 C, < 0.002 Sb, < 0.001 Al, and balance copper were used. The copper was phosphorus-deoxidized with a low residual phosphorus content (Type Cu-DLP, ISO 1337). The specimens, of $2.0 \times 2.0\,cm^2$, were mechanically cut from sheets 1.0 mm thick, and their surfaces were hand-polished with different grades of emery paper down to grade 600, degreased with acetone, rubbed energetically with cotton wool soaked in ethanol and finally dried at room temperature.

Table I indicates the composition of the simulated uterine fluid tested [15]. Reagent grade chemicals were used. Two pH values, 6.3 and 8.0, were tested. The pH value was adjusted by adding diluted reagent grade

TABLE I Composition of simulated uterine fluid (concentration, g/l)

$NaHCO_3$	$NaH_2PO_4 \cdot 2H_2O$	Glucose	NaCl	$CaCl_2$	KCl
0.25	0.072	0.50	4.97	0.167	0.224

hydrochloric acid or sodium hydroxide solution. Aerated solutions were tested; i.e. oxygen was not purged from the test solution. Experiments were carried out at $37.0 \pm 0.1\,^{\circ}C$ temperature.

Analyses were also carried out on copper-containing IUDs. The IUDs (Fig. 1) consisted of an inert plastic T-shaped matrix with a copper wire of 0.2 mm and two copper tabs of dimensions $5.0 \times 3.5\,mm^2$ and 0.2 mm thick (see magnified inset in Fig. 1). The chemical composition of the copper on the IUD was similar to that of the copper specimens immersed in simulated uterine fluid.

The commercial IUD was placed in a sealed and sterilized plastic bag and stored at room temperature for a period of 30 months. After this time the color of the copper had changed from the original red color to a dark color.

X-ray photo-electron spectroscopy (XPS) experiments were conducted using a VG Microtech Model MT 500 spectrophotometer with an $MgK_{\alpha 1,2}$ anode X-ray source ($h\nu = 1253.6$ eV), with a primary beam energy of 15 kV and an electron current of 20 mA. The pressure in the analysis chamber was maintained at 1×10^{-9} torr throughout the measurements. The regions of interest were Cu 2p, O 1s, S 2p, C 1s, Cl 2p, Ca 2p, P 2p and the Auger peak Cu(LMM). The instrumentation was periodically calibrated using Ag $3d_{5/2}$ (368.0 eV) and Au $4f_{7/2}$ (84.0 eV) substrates.

Argon ion sputtering was carried out to characterize the element composition using a primary beam energy of 5 kV and an ion intensity of 1 μA, recording in each sputtering the corresponding spectrum. The sputtering rate was obtained by ion etching of a Ta specimen covered by a Ta_2O_5 layer of known thickness. A copper etching rate of 10 Å/min was obtained, approximately 2.0 times faster than Ta_2O_5 [16].

Scanning electron microscopy (SEM) and energy dispersive X-ray (EDX) techniques were applied to observe the morphology and to identify the composition of the corrosion products originated, respectively, using a JEOL JXA-840 equipped with a LINK AN 10 000 system. Conducting specimens for SEM were prepared by graphite sputtering the copper specimens.

3. Results and discussions

3.1. Copper-containing IUDs

Figs 2 and 3 show XPS spectra for an uncorroded copper-containing IUD (used for comparative purposes) and a corroded copper-containing IUD, respectively. Spectrum S 2p is magnified in the inset of Fig. 3. The spectra were recorded on copper specimens in as-received state and after Ar^+ ion sputtering for 0.5 and 1.0 min. Some differences can be observed between the Cu $2p_{3/2}$ signals for the uncorroded (Fig. 2) and corroded (Fig. 3) copper IUD specimens. In the former, copper hydroxide ($Cu(OH)_2$) can be observed as the main component at ~ 934.5 eV along with a cuprite (Cu_2O) peak at ~ 932.5 eV in the as-received spectrum. After Ar^+

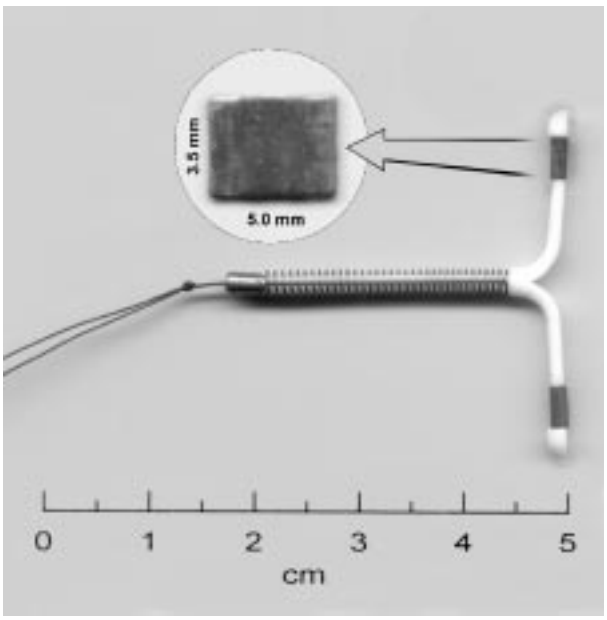

Figure 1 Copper-containing IUD tested.

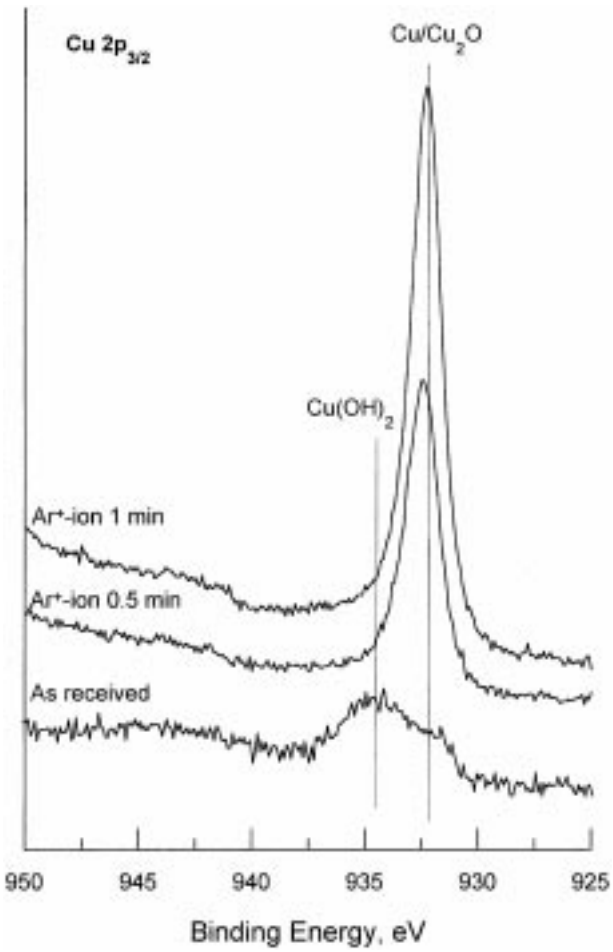

Figure 2 High resolution $Cu2p_{3/2}$ peaks for uncorroded copper IUD.

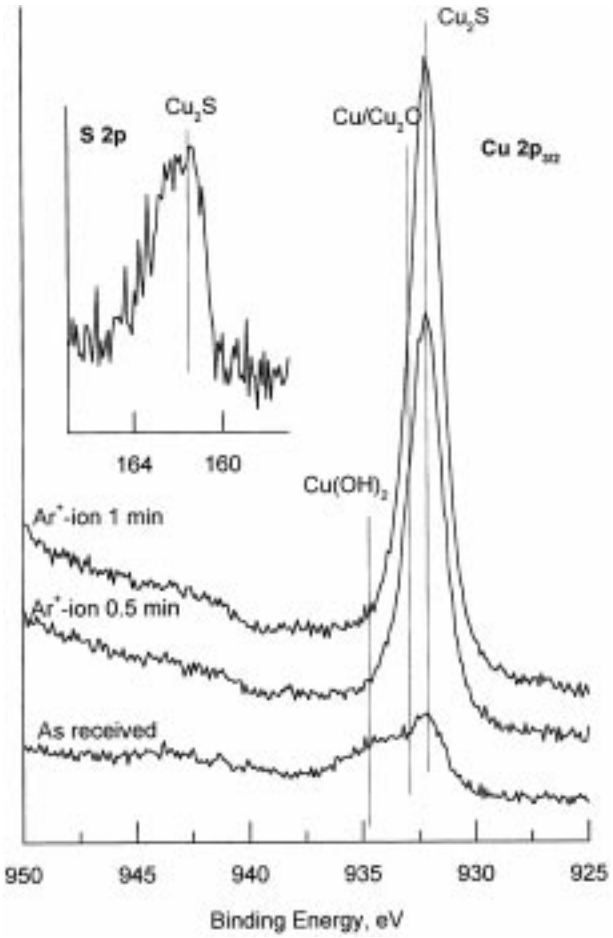

Figure 3 High resolution $Cu2p_{3/2}$ peaks for corroded copper IUD.

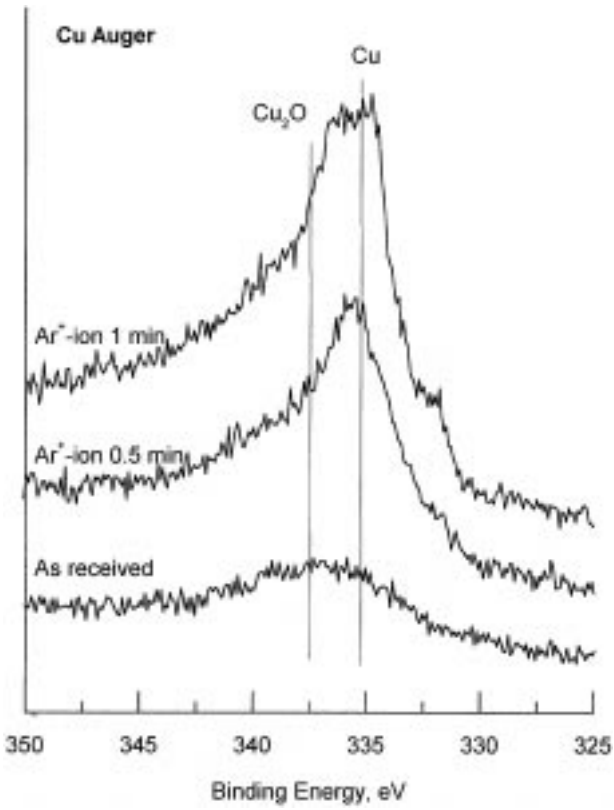

Figure 4 Cu Auger peaks for uncorroded copper IUD.

ion sputtering for 0.5 min, copper hydroxide disappears and a narrow peak corresponding to cuprite and/or metallic copper remains. In contrast with the corroded copper IUD specimens (Fig. 3), the contribution of sulphur compounds is the most important feature, it being possible to observe a CuS/Cu_2S peak at ~ 932.0 eV, as well as a small Cu/Cu_2O shoulder for 0.5 and 1.0 min Ar^+ ion sputtering. The contribution of $Cu(OH)_2$ is of little importance (see Fig. 3) and, as in the uncorroded IUD specimen disappears after 0.5 min Ar^+ ion sputtering. The S 2p peak in the inset of Fig. 3 is located at ~ 161.5 eV, indicating that the dark layer formed on the corroded copper IUD is mainly chalcocite (Cu_2S) [17]. It should be noted that the source of sulphur may be indoor contamination, though plastic materials are also a source of volatile organic compound contamination [18, 19] and poor sealing of the plastic bag may also facilitate copper corrosion.

Fig. 4 shows Cu(LMM) Auger electron peaks for an uncorroded copper IUD specimen in as-received state and after Ar^+ ion sputtering for 0.5 and 1.0 min. It can be observed that as sputtering time increased the contribution of metallic Cu became higher, with only a small contribution from the cuprite remaining. These results indicate that the surface patina on the uncorroded copper IUD is formed mainly by a cuprite layer of a little more than 10 Å thick.

Fig. 5 shows Cu(LMM) Auger peaks for a corroded copper IUD specimen in as-received state and after Ar^+ ion sputtering for 0.5 and 1.0 min. In contrast with Fig. 4, the contribution of metallic Cu is not observed. Fig. 5

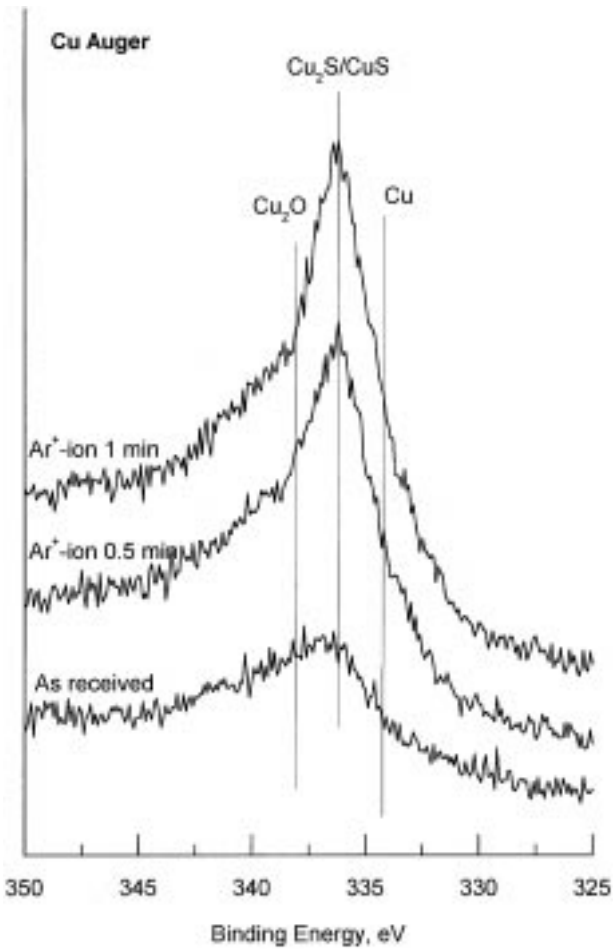

Figure 5 Cu Auger peaks for corroded copper IUD.

indicates that the surface patina on a corroded copper IUD specimen is mainly formed by copper sulphide compounds. The corroded layer of dark color was removed after 10 min bombardment with Ar^+ ions (this result was not included in Fig. 5). The thickness of the cuprite and copper sulphide layer may be estimated from the sputter rate of the ion gun to be approximately of 100 Å.

Fig. 6 shows the morphological aspect of uncorrected (Fig. 6(a)) and corroded (Fig. 6(b)) copper IUD specimens obtained by SEM along with the corresponding EDX spectra. A scratched surface can be observed on Fig. 6(a). On the corroded copper IUD specimen, Fig. 6(b), copper corrosion products with a flake-like shape can be observed, which the EDX spectrum shows Cu and S signals.

With regard to the corrosion process on the copper-containing IUD, it may be interpreted that the layer of dark color formed on corroded copper IUD specimens has a mixed structure consisting of an outer layer of chalcocite of matt black color and an inner layer of cuprite of red color [12]. The chalcocite layer does not seem to grow at the expense of the cuprite layer [18].

The porous nature of cuprite is known [19], and accordingly copper ions may diffuse from the copper surface to the outer corrosion product layer through faults and/or pores in the cuprite. However, even though the copper sulphide is also of porous nature [20], the stratified mixed structure of the corrosion product layer formed on the corroded copper IUD surface may obstruct the release of copper ions. It is concluded that the anti-fertility effectiveness of a corroded copper-containing IUD may be diminished.

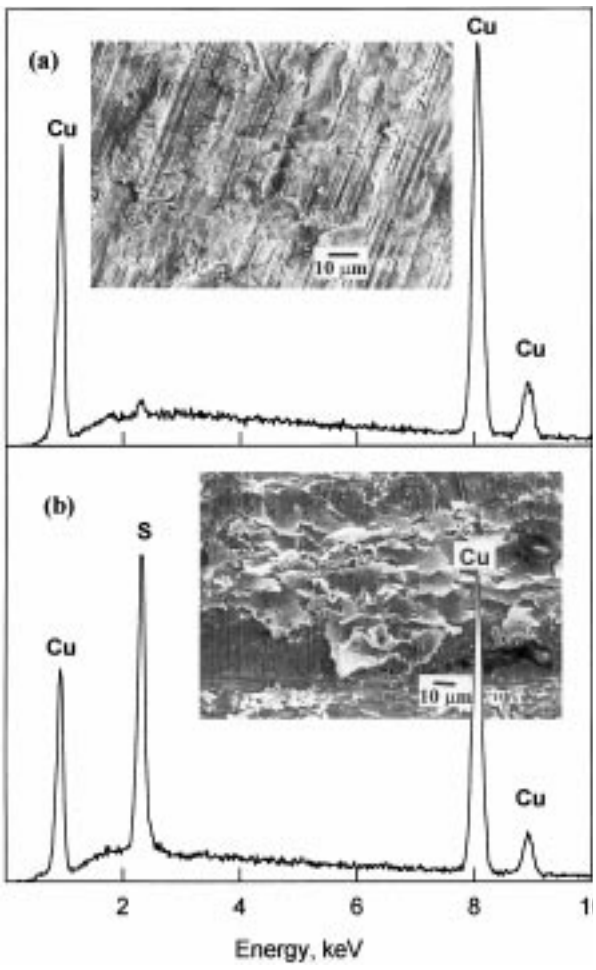

Figure 6 SEM micrographs and EDX spectra for (a) uncorroded copper IUD, and (b) corroded copper IUD.

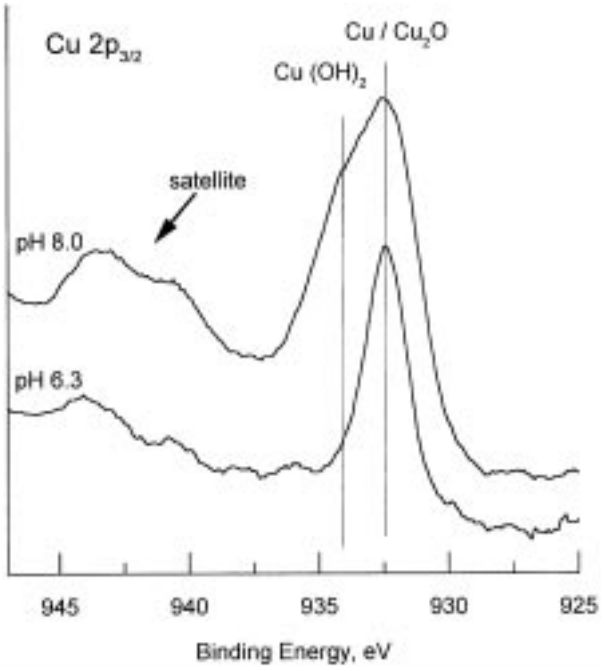

Figure 7 XPS spectra for copper immersed in simulated uterine fluid after 1 week experimentation.

3.2. Copper immersion in simulated uterine fluids

Fig. 7 shows XPS spectra for copper specimens after 1 week of immersion in simulated uterine fluids at two pH values, 6.3 and 8.0. The higher the pH, the greater the contribution of copper hydroxide (see Fig. 7). This behavior may be associated with the formation of a passive layer.

Fig. 8 shows depth profiles for copper specimens after 1 week of immersion in simulated uterine fluids at two pH values, Fig. 8(a) for pH 6.3 and Fig. 8(b) for pH 8.0. Fig. 8(a) shows the presence of chlorine-containing compounds, probably a CuCl layer, on the copper surface [21]. Fig. 8(a) also shows that oxygen compounds, probably as oxides and hydroxides, decreased as sputtering time increased, while at the same time the copper signal increased, indicating a higher uncovered copper surface exposed to the action of the artificial uterine solution. In contrast, Fig. 8(b) for pH 8.0 indicates that oxygen compounds increased with the sputtering time, probably as carbonate and phosphate deposits. At this pH value chlorine compounds were not observed.

Fig. 9 shows SEM and EDX results for copper immersed for 1 week in the simulated uterine solution at pH 6.3. It is possible to observe the formation of a cuprite layer on the copper surface and some corrosion protuberances of white color, whose composition is indicated in the spectrum. Chlorine is seen to be the main element detected, and Ca, Na, Si, P and K can also be observed.

Fig. 10 shows SEM and EDX results for copper specimens immersed for one week in the simulated uterine solution at pH 8.0. This figure corroborates the

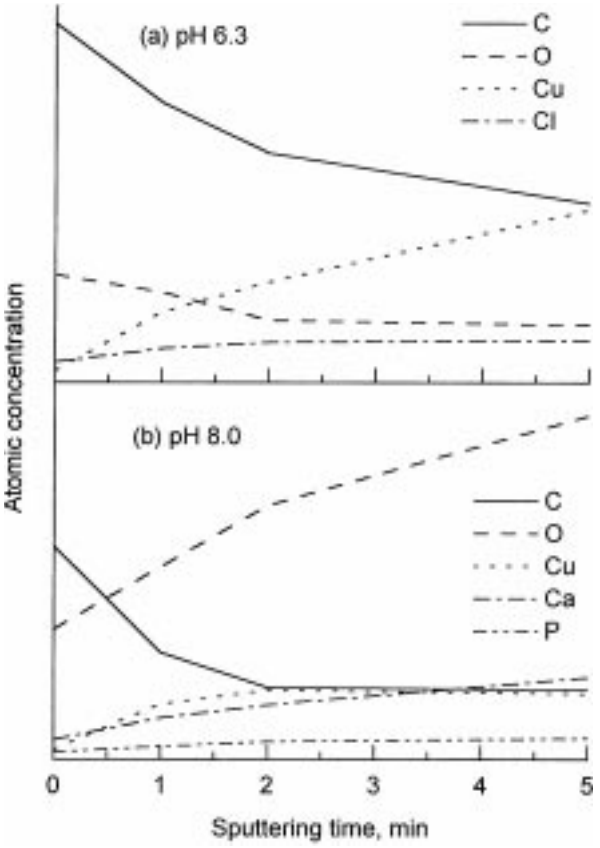

Figure 8 Compositional depth profile for copper immersed in simulated uterine fluid after 1 week experimentation, (a) pH 6.3, and (b) pH 8.0.

XPS results of Fig. 8(b). Over the cuprite layer, labeled (a) in the figure, a dark, compact and adherent layer was formed, labeled (b), which has the composition shown in the EDX spectrum. The presence of P, Ca, Si and Cl can be observed, with the latter as a minor contributor. The fact that chlorine was not found by the XPS method does not exclude its presence, and this result may indicate that chlorine compounds are located in a deeper layer.

Fig. 11 shows XPS spectra for copper specimens immersed for 12 weeks in the simulated uterine fluid at pH 6.3. Copper specimens immersed in the solution of pH 8.0 show similar behavior, and for this reason their results were not included. The spectra shows a peak

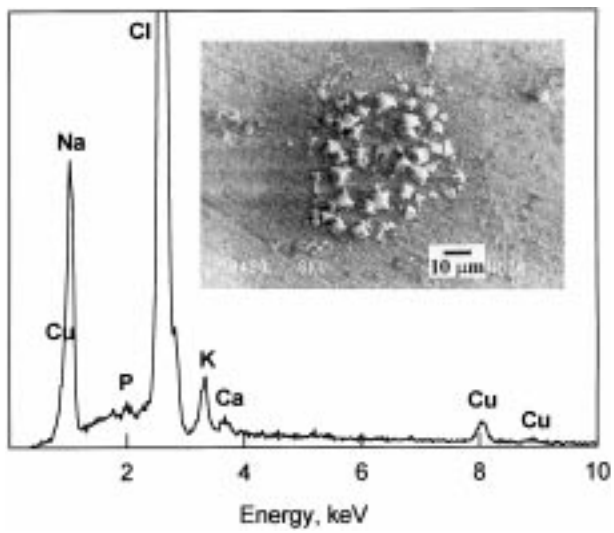

Figure 9 SEM micrograph and EDX spectrum for copper immersed in simulated uterine fluid at pH 6.3 after 1 week experimentation.

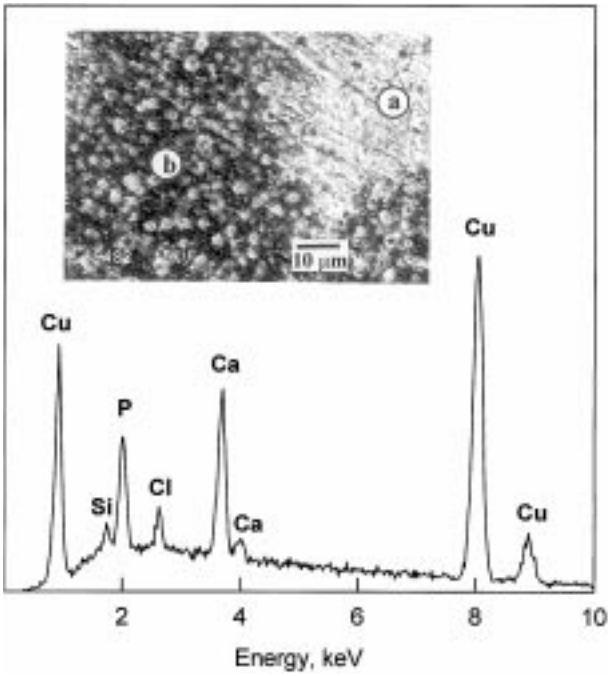

Figure 10 SEM micrograph and EDX spectrum for copper immersed in simulated uterine fluid at pH 8.0 after 1 week experimentation.

doublet which may be attributed to a differential charging process [22]. A displacement of the peaks is observed, originated by the non-conductive properties of the corrosion product layer deposited on the copper surface (see the inset figure). As sputtering time increased the uncovered copper surface became greater, as is indicated in the figure by a major contribution of the metallic copper peak (unshifted peak).

Fig. 12 shows depth profiles for copper specimens after 12 weeks of immersion in simulated uterine fluids

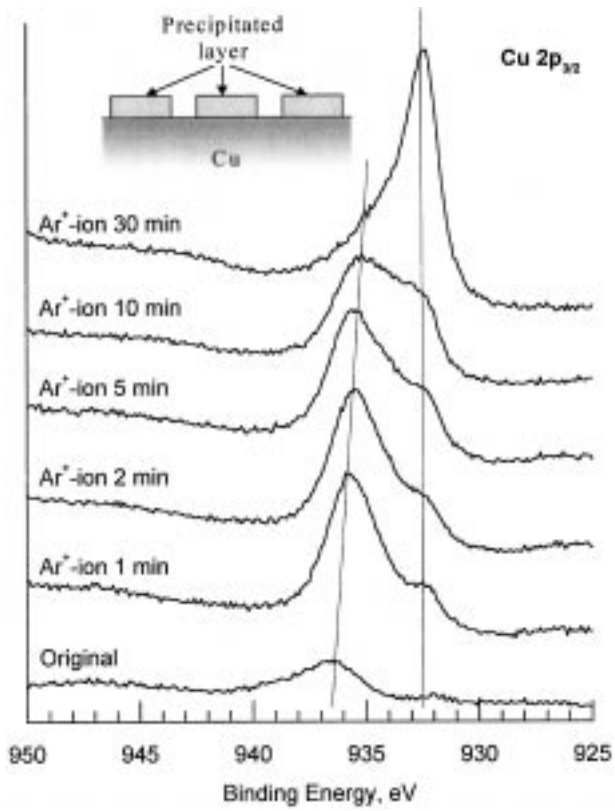

Figure 11 XPS spectra for copper immersed in simulated uterine fluid at pH 6.3 and after 12 weeks experimentation.

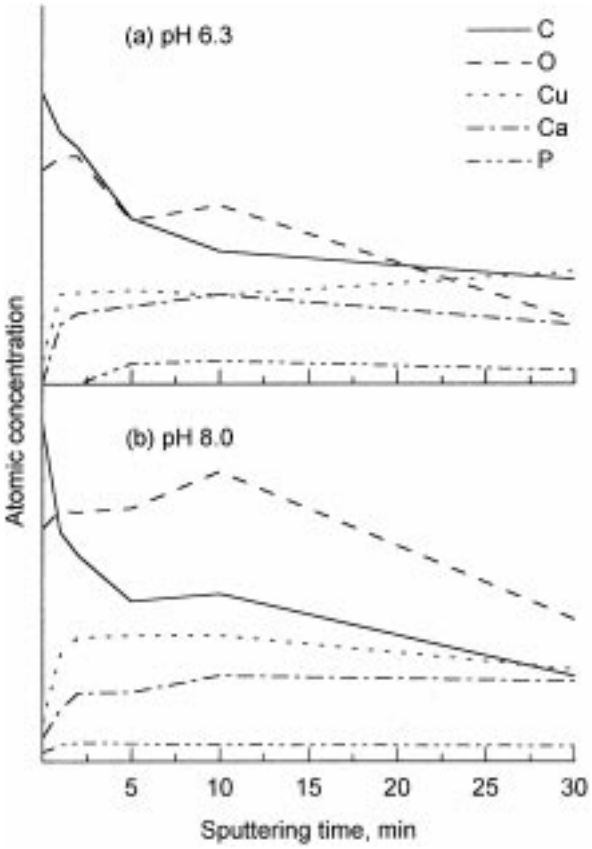

Figure 12 Compositional depth profile for copper immersed in simulated uterine fluid after 12 weeks experimentation, (a) pH 6.3, and (b) pH 8.0.

and at two pH values, Fig. 12(a) for pH 6.3 and Fig. 12(b) for pH 8.0. Fig. 12 shows that after 12 weeks experimentation the behavior for both pH values studied was similar. The differences observed at the early stages (1 week of immersion), Fig. 8, disappear after longer times (12 weeks). The corrosion product layer deposited probably obstructs the release of copper ions. After Ar^+ ion sputtering for 30 min the atomic % of Ca (corresponding to $CaCO_3$) and P (corresponding to calcium phosphate) remains constant, indicating that the carbonate/phosphate layer has a thickness of more than 300 Å.

Finally, Figs 13 and 14 show SEM and EDX results for copper specimens immersed for 12 weeks in simulated uterine solutions at pH 6.3 and 8.0, respectively. A cuprite layer can be observed in both Figs 13 and 14, Si, P, Cl and Ca signals can also be observed. Like Figs 9 and 10, these figures indicate that the copper corrosion layer is non-uniform, which may facilitate the release of copper ions.

4. Conclusions

X-ray photo-electron spectroscopy, scanning electron microscopy and energy dispersive X-ray measurements were performed to study the corrosion products originated on copper in simulated uterine fluids at two pH values 6.3 and 8.0.

The main components of the corrosion products originated were cuprite, chalcocite, calcite and phosphate compounds. The experimental results show the influence of pH on the copper corrosion process at the first stages of experimentation (1 week), indicated by the presence of

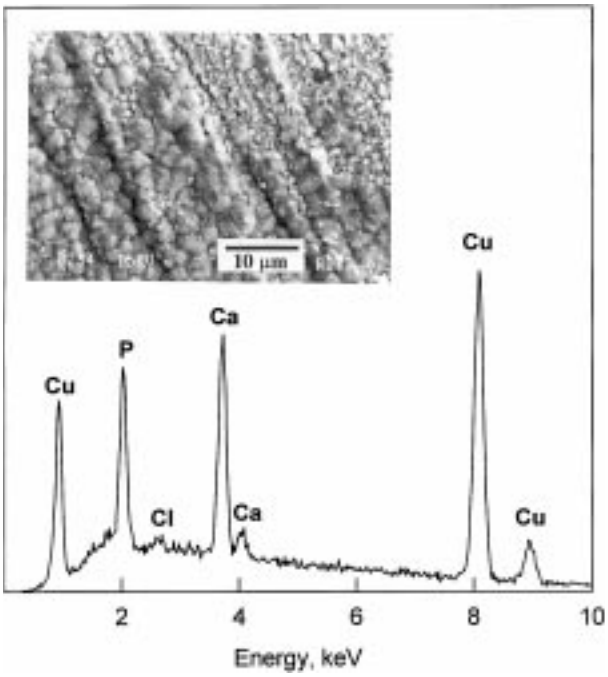

Figure 13 SEM micrograph and EDX spectrurn for copper immersed in simulated uterine fluid at pH 6.3 after 12 weeks experimentation.

chlorine compounds and oxygen as oxide and hydroxide species. However, after 12 weeks' experimentation the pH level was not seen to influence the experimental results. The morphology of the corrosion products was a non-uniform layer which allows the release of copper ions.

The thin dark colored layer of corrosion products formed on copper-containing IUD specimens stored at room temperature for a period of 30 months was composed of an outermost layer of chalcocite (Cu_2S) and an inner layer of cuprite (Cu_2O). On uncorroded copper IUD specimens the original red color film formed on the copper was cuprite. Copper corrosion phenomenon may reduce the anti-fertility effectiveness of a copper-containing IUD.

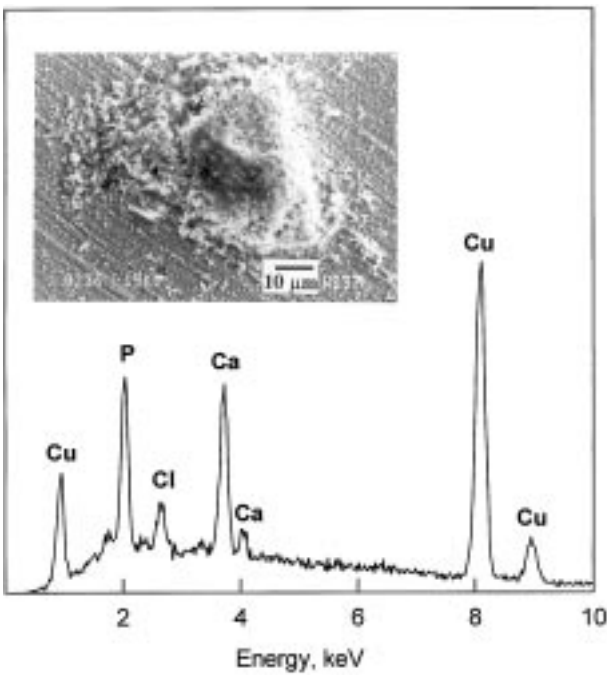

Figure 14 SEM micrograph and EDX spectrum for copper immersed in simulated uterine fluid at pH 8.0 after 12 weeks experimentation.

Acknowledgment

E. Cano expresses his gratitude to the Spanish Ministry of Education and Culture for the scholarship granted to him.

References

1. G. OSTER and M. P. SALGO, *New Engl. J. Med.* **28** (1975) 432.
2. G. K. OSTER, *Fertil Steril.* **23** (1972) 18.
3. W. A. A. VAN OS, C. C. A. DE NOOYER and P. E. R. RHEMREV, in ''Medicated Intrauterine Devices Physiological and Clinical Aspects'' (Martinus Nijhoff, London, 1980) p. 111.
4. K. HAGENFELDT, *Contraception* **6** (1972) 37.
5. H. TIMONEN, *Contraception* **14** (1976) 25.
6. A. KOSONEN, *Fertil. Steril.* **30** (1978) 59.
7. H. H. EL-BADRAWI and E. S. E. HAFEZ, in ''Medicated Intrauterine Devices Physiological and Clinical Aspects'' (Martinus Nijhoff, London, 1980) p. 60.
8. A. KOSONEN, in ''Medicated Intrauterine Devices Physiological and Clinical Aspects'' (Martinus Nijhoff, London, 1980) p. 22.
9. M. THIERY, F. SCHMIDT and H. J. TATUM. *Contraception* **26** (1982) 295.
10. R. W. JONES, N. M. GREGSON and M. ELSTEIN, *Brit. Med. J.* **2** (1973) 520.
11. A. SEDLIS, E. KANDEMIR and M. L. STONE, *Obstet. Gynecol.* **30** (1967) 114.
12. H. LEIDHEISER JR., in ''The Corrosion of Copper, Tin, and Their Alloys'' (Wiley, New York, 1971) p. 14 and p. 60.
13. J. M. BASTIDAS, A. LOPEZ-DELGADO, F. A. LOPEZ and M. P. ALONSO, *J. Mater. Sci.* **32** (1997) 129.
14. J. M. BASTIDAS and J. SIMANCAS. *Biomaterials* **18** (1997) 247.
15. C. ZHANG, N. XU and B. YANG, *Corros. Sci.* **38** (1996) 635.
16. B. I. RICKETT and J. H. PAYER, *J. Electrochem. Soc.* **142** (1995) 3713.
17. S. K. CHAWLA, N. SANKARRAMAN and J. H. PAYER, *J. Electron Spectroc.* **61** (1992) 1.
18. A. LOPEZ-DELGADO, E. CANO, J. M. BASTIDAS and F. A. LOPEZ, *J. Electrochem. Soc.* **145** (1998) 4140.
19. D. W. RICE, R. J. CAPPELL, W. KINSOLVING and J. J. LASKOWSKI, *J. Electrochem. Soc.* **127** (1980) 891.
20. S. P. SHARMA, *J. Electrochem. Soc.* **127** (1980) 21.
21. A. MOREAU, *Electrochim. Acta* **26** (1981) 1609.
22. S. FELIU JR., J. L. G. FIERRO and C. MAFFIOTTE, *Prog. Org. Coat.* **30** (1997) 247.

Received 13 January
and accepted 14 January 2000